Supporting information

Sulfur poisoning mechanism of nanostructured Fe-Mn spinel catalysts for low-temperature NH_3-SCR

Yujia Tang[2], Jiaxiu Guo[1,3,4],* Xueke Shi[2], Xiaoxiong Liu[2]

1. College of Carbon Neutrality Future Technology, Sichuan University, Chengdu 610065, Sichuan, China

2. College of Architecture and Environment, Sichuan University, Chengdu 610065, China

3. National Engineering Research Center for Flue Gas Desulfurization, Chengdu 610065, China

4. Industrial Technology Research Institute, Sichuan University, Yibin, 644004, China

*Corresponding author: Jiaxiu Guo; E-mail: guojiaxiu@scu.edu.cn (J. Guo).

Text A

X-ray diffraction (XRD) patterns were recorded on a Rigaku Ultima IV diffractometer using Cu Kα radiation (40 kV, 40 mA) over a 2θ range of 5–90° at a scan rate of 10°/min.

N_2 adsorption-desorption isotherms were measured at liquid N_2 temperature (−196°C) using a Micromeritics ASAP 2460 analyzer. Prior to measurement, samples were outgassed at 300°C. The specific surface area and pore size distribution of all catalysts were determined using the BET equation and BJH method, respectively.

X-ray photoelectron spectroscopy (XPS) was performed using a Thermo Scientific K-Alpha spectrometer with Al Kα radiation (hν = 1486.68 eV) as the excitation source to determine the binding energies of Fe 2p, Mn 2p, Mn 3s, S 2p and

O 1s. The C 1s line at 284.8 eV was used as a reference for binding energy calibration.

Thermogravimetric analysis (TGA) was conducted using a DSC-TGA instrument (TA Q600). Samples were heated under nitrogen atmosphere (60 mL/min) from room temperature to 950°C at a heating rate of 10°C/min.

Temperature-programmed characterization was performed using a chemisorption analyzer (VDSorb-91i, China) equipped with a thermal conductivity detector (TCD). For temperature-programmed reduction (H_2-TPR), approximately 100 mg of catalyst was loaded into a microreactor and pretreated under high-purity He at 300°C for 60 min, then cooled to 50°C. The gas was then switched to a 5% H_2/He mixture. After baseline stabilization, the catalyst was heated to 750°C at a heating rate of 10°C/min. H_2 consumption was monitored online by TCD using copper oxide as a standard. CuO was used as a standard to estimate H_2 consumption. The H_2 consumption is calculated as following:

$$H_2 \text{ consumption } = \frac{m_{CuO} \times A_{catalyst}}{M_{CuO} \times A_{CuO}}$$

Here, m_{CuO} is the quality of CuO; M_{CuO} is the molar mass of CuO; $A_{catalyst}$ is the H_2 consumption peak area of catalyst; and A_{CuO} is the H_2 consumption peak area of CuO.

Temperature-programmed desorption (TPD) experiments were conducted for NH_3, O_2, NO, and SO_2 (NH_3-TPD, O_2-TPD, NO-TPD, and SO_2-TPD). In a typical procedure, approximately 100 mg of catalyst was pretreated in high-purity He at 300°C for 1 h and then cooled to 50°C. The catalyst was then exposed to the respective gas mixture (1% NH_3/N_2 for NH_3-TPD, O_2 for O_2-TPD, 1% NO/N_2 for NO-TPD, or 0.1% SO_2/N_2 for SO_2-TPD) for 1 h, followed by purging with high-purity He (20 mL/min) to remove weakly adsorbed species. After baseline stabilization, the catalyst was heated from 50 to 750°C at a heating rate of 10°C/min. The effluent gas was analyzed using a dthermal conductivity detector (TCD).

In-situ diffuse reflectance infrared Fourier transform spectroscopy (in-situ DRIFTS) experiments were performed using a Nicolet iS50 FTIR spectrometer (Thermo Fisher Scientific) equipped with an MCT detector. For the SCR experiment, catalysts were pretreated with high-purity N_2 at 300°C for 1 h, then cooled to 120°C. The gas feeds used for the experiments were: 500 ppm NH_3/N_2, 500 ppm NO + 5 vol.% O_2/N_2, or 100 ppm SO_2 + 5 vol.% O_2/N_2.

Table S1 Cell parameters and Crystalline size of Catalysts.

Catalysts	Cell parameters (Å)			Crystalline size (nm)
	a	b	c	
Mn_3O_4	5.7598	5.7598	9.4520	43.1
$Fe_{0.2}Mn_{2.8}O_4$	5.7638	5.7638	9.4334	28.8
$Fe_{0.4}Mn_{2.6}O_4$	5.7615	5.7615	9.4275	27.0
$Fe_{0.6}Mn_{2.4}O_4$	5.7692	5.7692	9.3919	17.3
$Fe_{0.8}Mn_{2.2}O_4$	5.7678	5.7678	9.4044	16.8
$FeMn_2O_4$	5.7819	5.7819	9.3634	8.4
Mn_3O_4-120	5.7614	5.7614	9.4527	38.3
$Fe_{0.8}Mn_{2.2}O_4$-120	5.7676	5.7676	9.3863	16.9

Table S2 H_2 uptake form H_2-TPR.

Catalysts	Total H_2 uptake (mmol/g)
	150-650°C
Mn_3O_4	1.39
$Fe_{0.8}Mn_{2.2}O_4$	1.47

Table S3 The peak areas of Mn_3O_4 and $Fe_{0.8}Mn_{2.2}O_4$ from NO-TPD, O_2-TPD and SO_2-TPD.

Catalysts	NO-TPD		O_2-TPD	SO_2-TPD
	80-300°C	300-600	<300°C	80-750°C
Mn_3O_4	369.34	403.95	211.68	1153.20
$Fe_{0.8}Mn_{2.2}O_4$	444.36	711.72	231.56	2974.90

Table S4 The peak areas of Mn_3O_4, Mn_3O_4-120, $Fe_{0.8}Mn_{2.2}O_4$ and $Fe_{0.8}Mn_{2.2}O_4$-120 from NH_3-TPD.

Catalysts	NH_3-TPD	
	80-300℃	300-600℃
Mn_3O_4	107.93	310.23
Mn_3O_4-120	84.13	193.32
$Fe_{0.8}Mn_{2.2}O_4$	281.60	403.10
$Fe_{0.8}Mn_{2.2}O_4$-120	186.03	541.94

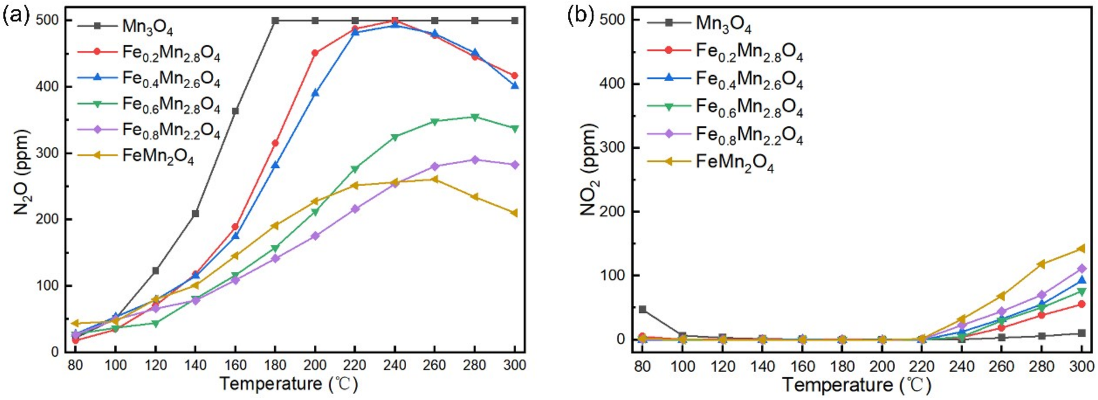

Fig. S1 (a) Concentration of N_2O and (b) NO_2 produced.

Fig. S2 TG curves of Mn_3O_4 (a), $Fe_{0.8}Mn_{2.2}O_4$ (b), Mn_3O_4-120 (c), $Fe_{0.8}Mn_{2.2}O_4$ (d).

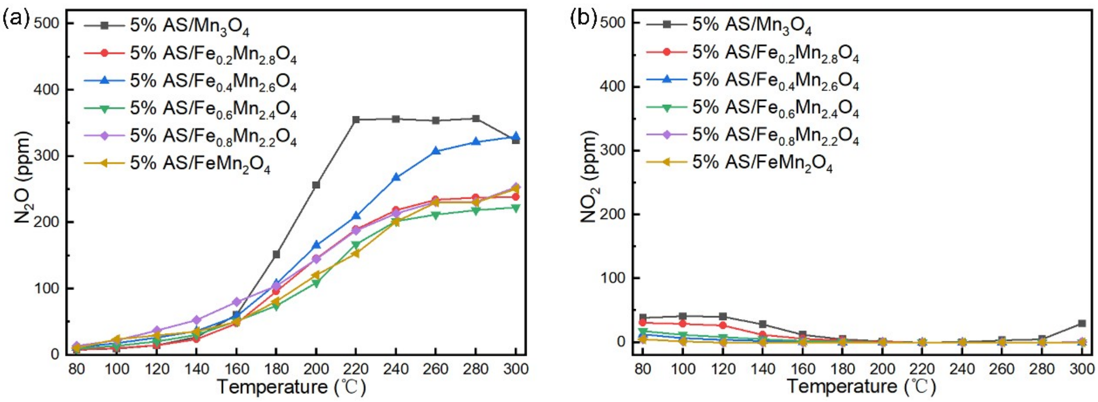

Fig. S3 (a) Concentration of N_2O and (b) NO_2 produced

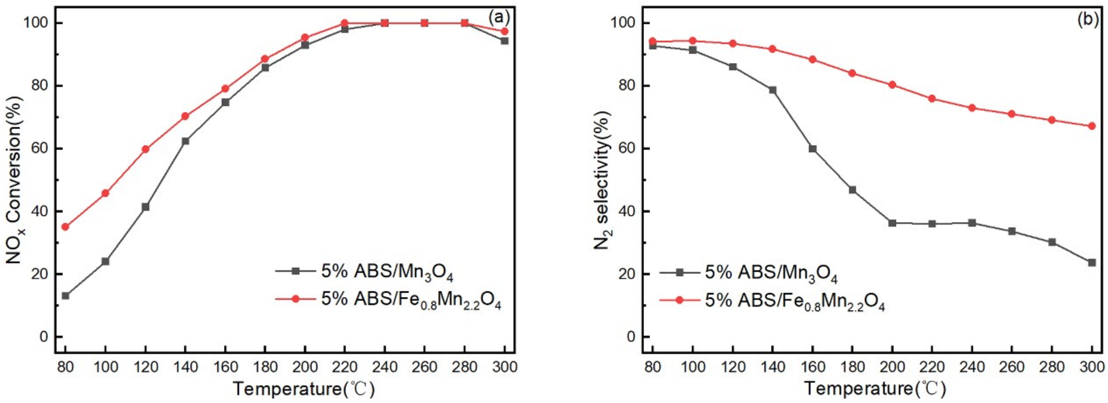

Fig. S4 (a) NH_3-SCR activity; (b) N_2 selectivity; Reaction condition: 500 ppm NO, 500 ppm NH_3, 5 vol% O_2 and balance as N_2; A total flow rate of 500 mL/min and GHSV at 30, 000 h^{-1}.

The results are similar to those observed with AS deposition. Compared with pure Mn_3O_4, $Fe_{0.8}Mn_{2.2}O_4$ exhibits improved low-temperature activity and enhanced high-temperature N_2 selectivity.

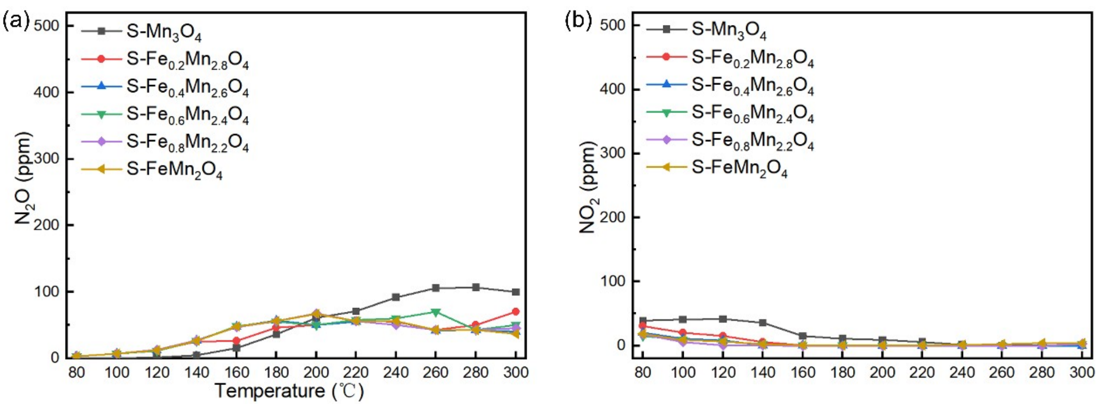

Fig. S5 (a) Concentration of N_2O and (b) NO_2 produced.

Fig. S6 TG curves of 5%ABS/Mn_3O_4 (a), S-Mn_3O_4 (c), 5%ABS/$Fe_{0.8}Mn_{2.2}O_4$ (b) and S-$Fe_{0.8}Mn_{2.2}O_4$ (d).

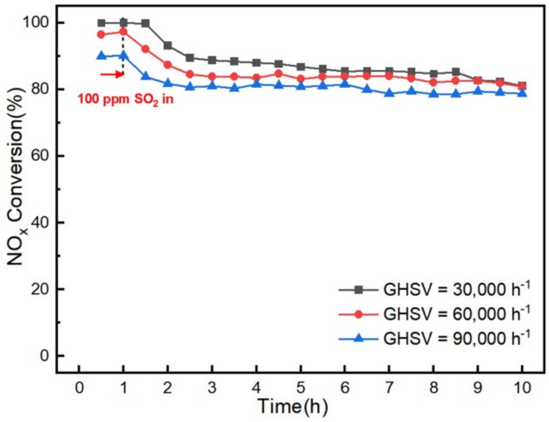

Fig. S7. SO_2 resistance lifetime test of the $Fe_{0.8}Mn_{2.2}O_4$ catalyst at 120 °C under high GHSV.

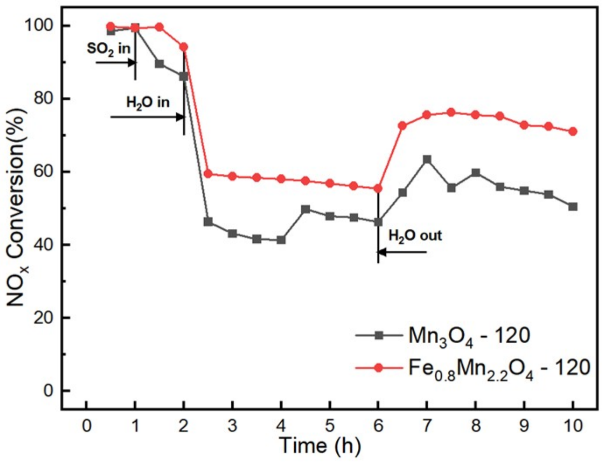

Fig. S8 Effect of H_2O on NO_x conversion over Mn_3O_4 and $Fe_{0.8}Mn_{2.2}O_4$ at 120 °C. Reaction conditions: 500 ppm NO, 500 ppm NH_3, 5% O_2, 100 ppm SO_2 (when used), 10% H_2O (when used), N_2 balance, GHSV = 30,000 h^{-1}.

The effect of H_2O on catalytic performance was evaluated at 120 °C under the following sequence: 1-10 h with 100 ppm SO_2, 2-6 h with 10 vol% H_2O, and 6-10 h without H_2O (Fig. S8). $Fe_{0.8}Mn_{2.2}O_4$ exhibited superior water tolerance, maintaining 55% conversion at 6 h and rapidly recovering to 71% upon H_2O removal. In contrast, Mn_3O_4 dropped to 46% at 6 h and only recovered to 50% at 10 h, indicating irreversible deactivation by water vapor.

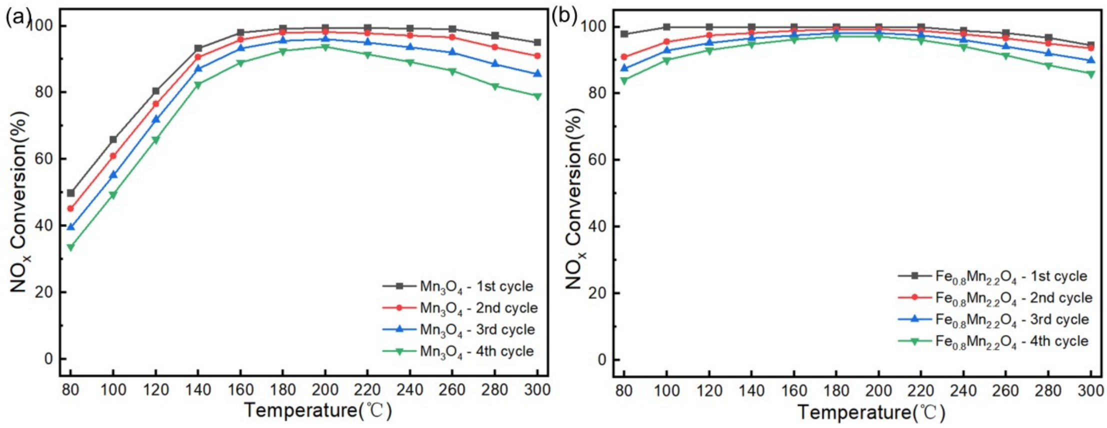

Figure S9. Cycling stability tests over four consecutive cycles: (a) Mn_3O_4, (b) $Fe_{0.8}Mn_{2.2}O_4$. Reaction conditions: 500 ppm NO, 500 ppm NH_3, 5% O_2, N_2 balance, GHSV = 30,000 h^{-1}, temperature range 80-300 °C.

Cycling stability was evaluated over four consecutive cycles (80-300 °C) with N_2 purge between cycles (Figs. S9). $Fe_{0.8}Mn_{2.2}O_4$ showed stable performance with minimal deactivation, while Mn_3O_4 exhibited more pronounced activity loss, confirming the beneficial role of Fe doping in enhancing catalyst durability.

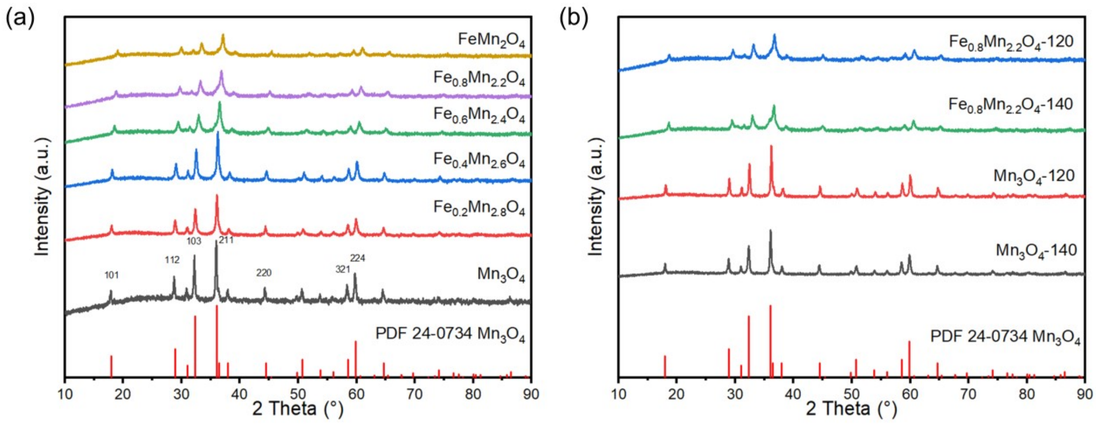

Fig. S10 (a) XRD patterns of $Fe_xMn_{3-x}O_4$ catalysts (b) XRD patterns of Mn_3O_4-120, Mn_3O_4-140, $Fe_{0.8}Mn_{2.2}O_4$-120 and $Fe_{0.8}Mn_{2.2}O_4$-140.

Fig.S10 (a) shows the XRD patterns of the $Fe_xMn_{3-x}O_4$ catalysts. It can be found that all samples exhibit good correspondence with the hausmannite Mn_3O_4 phase (JCPDS: #24-0734). Fig. S8(b) shows the XRD patterns of Mn_3O_4 and $Fe_{0.8}Mn_{2.2}O_4$ tested at 140 °C and 120 °C. After 9 hours of SCR reaction with SO_2 at different temperatures, no diffraction peaks belonging to sulfate species were observed. This indicates that no bulk sulfate species have formed, and the sulfate species are highly dispersed or exist as very small particles on the catalyst surface.

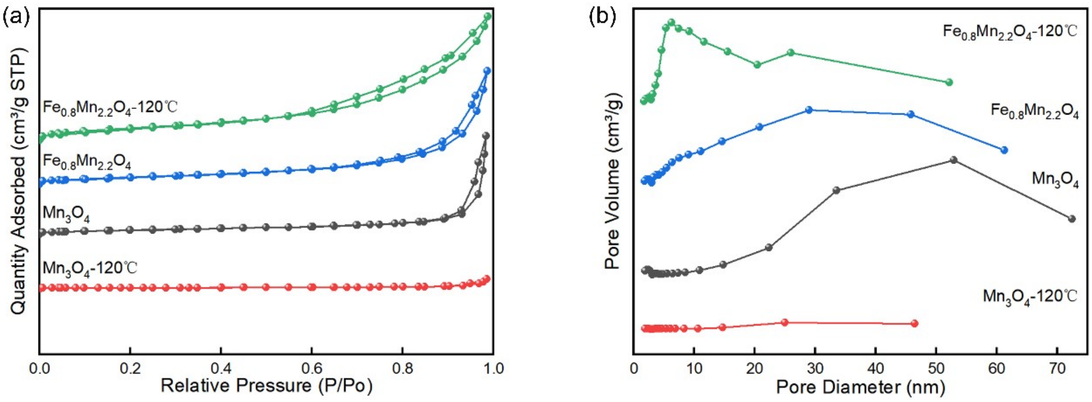

Fig. S11 Nitrogen adsorption-desorption curves; (b) Pore size distribution curves.

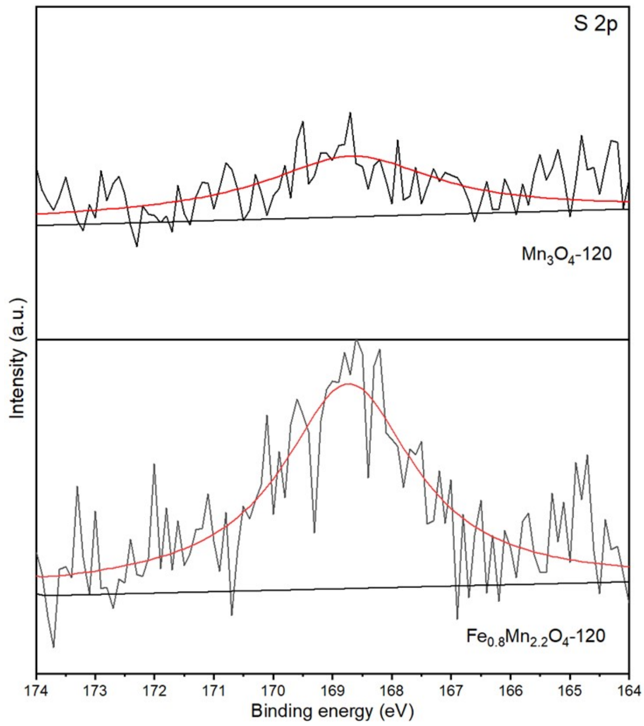

Fig. S12 XPS S 2p spectra of sulfated catalysts.

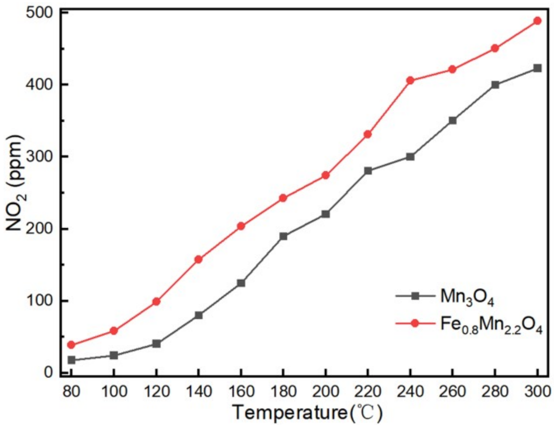

Fig. S13 NO oxidation performance over Mn_3O_4 and $Fe_{0.8}Mn_{2.2}O_4$ catalysts.